Supplemental Material: Random-gate-voltage induced Al'tshuler-Aronov-Spivak effect in topological edge states

Kun Luo,[1] Wei Chen,[1,2,*] Li Sheng,[1,2] and D. Y. Xing[1,2]

[1] *National Laboratory of Solid State Microstructures and school of Physics, Nanjing University, Nanjing, 210093, China*
[2] *Collaborative Innovation Center of Advanced Microstructures, Nanjing University, Nanjing 210093, China*

(Dated: September 29, 2021)

I. LATTICE MODEL FOR NUMERICAL CALCULATION

Here, we elucidate the parameters for the interferometer sketched in main text Fig. 1(a). The hard-wall boundary in the y direction is described by the following function

$$|y(x)| = \begin{cases} \left(W-(W-W_{PC}e^{-(x+L_M/2+L_{PC})^2/30^2})\right)/2, & -L<x<-(L_M/2+L_{PC}), \\ W_{PC}/2, & -(L_M/2+L_{PC})\le x\le -L_M/2, \\ \left(W-(W-W_{PC}e^{-(x+L_M/2)^2/30^2})\right)/2, & -L_M/2<x<0, \\ \left(W-(W-W_{PC}e^{-(x-L_M/2)^2/30^2})\right)/2, & 0\le x<L_M/2, \\ W_{PC}/2, & L_M/2\le x\le (L_M/2+L_{PC}), \\ \left(W-(W-W_{PC}e^{-(x-L_M/2-L_{PC})^2/30^2})\right)/2, & (L_M/2+L_{PC})<x<L, \end{cases} \tag{1}$$

where W is the width of the lead, W_{PC} and L_{PC} are the width and length of PC.

The whole devices can be described by Hamiltonian $H = H_{QSH} + H_R$, where H_{QSH} is the Hamiltonian of QSHI and H_R is the Hamiltonian of SOC. Here, we use HgTe/CdTe quantum wells in our proposal, which can be described by Bernevig-Hughes-Zhang model as

$$\begin{aligned} H_{QSH} &= -Dk^2 + Ak_x\tau_x\sigma_z - Ak_y\tau_y + (M-Bk^2)\tau_z \\ &= \begin{pmatrix} D_k+M_k & Ak_+ & 0 & 0 \\ Ak_- & D_k-M_k & 0 & 0 \\ 0 & 0 & D_k+M_k & -Ak_- \\ 0 & 0 & -Ak_+ & D_k-M_k \end{pmatrix}, \end{aligned}$$

where $\sigma_{x,y,z}$ and $\tau_{x,y,z}$ are Pauli matrices of spin and orbital respectively. $k_\pm = k_x \pm ik_y$, $k^2 = k_x^2 + k_y^2$, $D_k = -Dk^2$, and $M_k = M - Bk^2$. A, B, D and M are the material parameters which can be controlled by experiment. The Hamiltonian of SOC is

$$\begin{aligned} H_R &= 0.5\alpha(1+\tau_z)(k_x\sigma_y - k_y\sigma_x) \\ &= \begin{pmatrix} 0 & 0 & -i\alpha k_- & 0 \\ 0 & 0 & 0 & 0 \\ i\alpha k_+ & 0 & 0 & 0 \\ 0 & 0 & 0 & 0 \end{pmatrix}, \end{aligned}$$

where α is Rashba coefficient.

In order to run numerical calculations, we use a square lattice model for whole system by discretizing the continuous effective hamiltonian H. By using $k^2 = 2a^{-2}[2-\cos(k_xa)-\cos(k_ya)]$, $k_x = a^{-1}\sin(k_xa)$, $k_y = a^{-1}\sin(k_ya)$, we can derive the Hamiltonian to real space. The lattice Hamiltonian is

$$\begin{aligned} H = &\sum_{i=1} c_i^\dagger H_{ii} c_i + \sum_{i=1} c_i^\dagger H_{i,i+a_x} c_{i+a_x} \\ &+ \sum_{i=1} c_i^\dagger H_{i,i+a_y} c_{i+a_y} + H.C., \end{aligned} \tag{2}$$

where $c_i = (c_{s,\uparrow,i}, c_{p,\uparrow,i}, c_{s,\downarrow,i}, c_{p,\downarrow,i})$ are the annihilate operators of electron with spin up and spin down in s and p orbits at site i. The H_{ii}, $H_{i,i+a_x}$ and $H_{i,i+a_y}$ are 4×4 Hamiltonians,

$$\begin{aligned} H_{ii} &= -\frac{4D}{a^2} - \frac{4B}{a^2}\tau_z + M\tau_z, \\ H_{i,i+a_x} &= \frac{D+B\tau_z}{a^2} + \frac{A\tau_x\sigma_z}{2ia} + \frac{\alpha(1+\tau_z)\sigma_y}{4ia}, \\ H_{i,i+a_y} &= \frac{D+B\tau_z}{a^2} + \frac{iA\tau_y}{2a} + \frac{i\alpha(1+\tau_z)\sigma_x}{4a}, \end{aligned} \tag{3}$$

where lattice constant is $a = 3$nm. As a weak magnetic field is applied along $z-$direction, the nearest neighbour hopping T_{ij} should add a Peierls phase, $T_{ij}\times\exp(i\frac{e}{\hbar}\int_i^j \boldsymbol{A}\cdot$

* Corresponding author: pchenweis@gmail.com

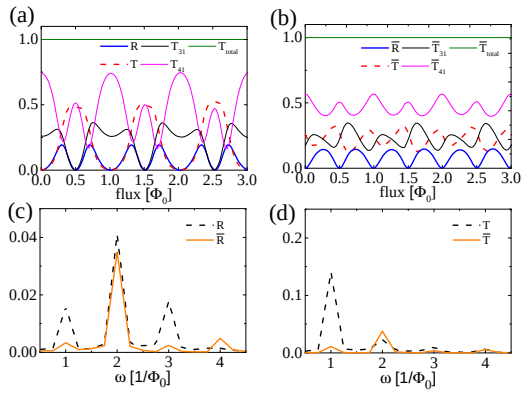

FIG. 1. Oscillation patterns of scattering probabilities by lattice simulation for (a) $V_g = 0$ and (b) random V_g with $\mathcal{W} =$ 10meV. The FFT spectrum of (c) the return probability $R(\bar{R})$ and (d) the transmission probability $T(\bar{T})$. All parameters are the same as those in main text Fig. 2 except for $\alpha_R = 180$ nm meV.

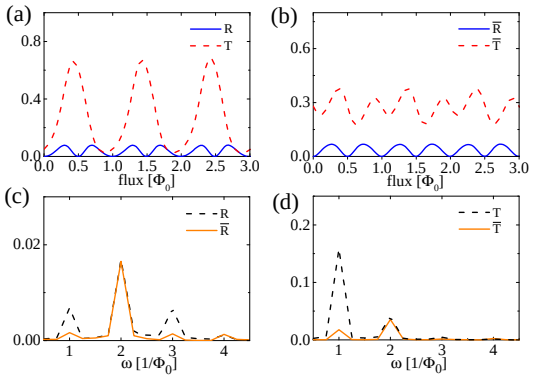

FIG. 2. Oscillation patterns of scattering probabilities and their FFT spectra. All parameters are the same as those in main text Fig. 2 except for $L_{RPC} = 180$ nm.

dr), where T_{ij} is the hopping for site i to site j. The vector potential is chosen as $\boldsymbol{A} = (-B_z y, 0, 0)$.

II. NUMERICAL RESULTS FOR DIFFERENT PARAMETERS

First, we change the Rashba coefficient α_R at the right PC. The scattering probabilities $T, R, T_{31}, T_{41}, T_{\text{total}}$ $(\bar{T}, \bar{R}, \bar{T}_{31}, \bar{T}_{41}, \bar{T}_{\text{total}})$ without (with) V_g averaging are shown in Fig. 1. One can see that the main results still hold, i.e., the random V_g quenches the Φ_0-period oscillation and leads to a dominant $\Phi_0/2$-period oscillation as shown in Figs. 1(a) and 1(b). There are three peaks in the frequency domain of R, and only a single peak at $2/\Phi_0$ survives in $\bar{R}$ after V_g averaging; see Fig. 1(c). Accordingly, the $\Phi_0/2$-period AAS oscillation overwhelms the Φ_0-period AB oscillation in the transmission

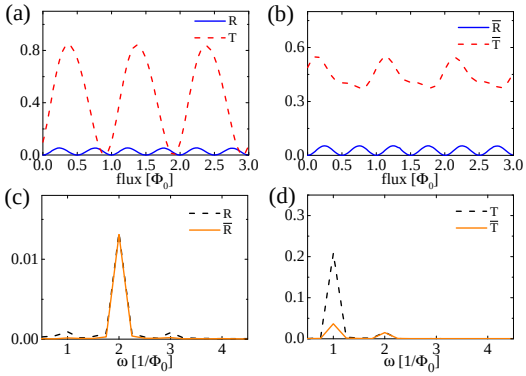

FIG. 3. Oscillation patterns of scattering probabilities and their FFT spectra. All parameters are the same as those in main text Fig. 2 except for a different incident energy of 2 meV.

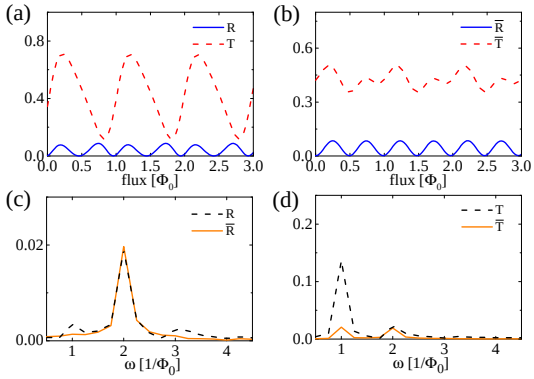

FIG. 4. Oscillation patterns of scattering probabilities and their FFT spectra with disorder strength 5 meV. All parameters are the same as those in main text Fig. 2.

probability $\bar{T}$ as shown in Fig. 1 (d). Similar results also hold as one varies the length L_{RPC} of the right PC as shown in Fig. 2. Fig. 3 shows the similar results with a different incident energy. The $\Phi_0/2$-period oscillation dominates the return probability (R and $\bar{R}$) before and after V_g averaging. The Φ_0-period oscillation of the transmission probability is strongly suppressed by the random V_g, while the $\Phi_0/2$ component remains unaffected. We also show in Fig. 4 that our results are robust against disorder. Since the main results are stabilized by the time-reversal symmetry, the modification of the sample details will not change the qualitative results. From Figs. 1-4, one can see that the averaged return probability $\bar{R}(\Phi = 0) = 0$ generally holds for various sample parameters, indicating the universality of the predicted signal of the helical edge states.